TURBULENT NATURAL-CONVECTION HEAT TRANSFER IN A SQUARE CAVITY WITH NANOFLUIDS IN PRESENCE OF INCLINED MAGNETIC FIELD

by

Mohamed EL HATTAB [a,b*] ***and Zakaria LAFDAILI*** [a]

[a] Mechanics, Process of Energy and Environment Laboratory, ENSA, Ibn Zohr University, Agadir, Morocco
[b] Research Team, Energy and Sustainable Development, ESTG, Ibn Zohr University, Guelmim, Morocco

Original scientific paper
https://doi.org/10.2298/TSCI210825326E

In this paper, we present a numerical study of turbulent natural-convection in a square cavity differentially heated and filled with nanofluid and subjected to an inclined magnetic field. The standard k-ε model was used as the turbulence model. The transport equations were discretized by the finite volume method using the SIMPLE algorithm. The influence of the Rayleigh number, the Hartmann number, the orientation angle of the applied magnetic field, the type of nanoparticles as well as the volume fraction of nanoparticles, on the hydrodynamic and thermal characteristics of the nanofluid was illustrated and discussed in terms of streamlines, isotherms and mean Nusselt number. The results obtained show that the heat transfer rate increases with increasing Rayleigh number and orientation angle of the magnetic field but it decreases with increasing Hartmann number. In addition, heat transfer improves with increasing volume fraction and with the use of Al_2O_3 *nanoparticles.*

Key words*: natural-convection, k-ε turbulence model, magnetic field, nanofluid*

Introduction

Nanofluids are solutions containing particles of nanometric size suspended in a base fluid, in order to improve its thermal properties. Thanks to their thermal performance, nanofluids can be used in several sectors, including domestic, engineering and biomedical. In the case of thermal convection within nanofluids, which are generally good conductors, both thermal and electrical, and in the presence of a magnetic field, the nanofluid is subjected to two volume forces: the buoyancy force and that of Lorentz. The latter can induce MHD. The study of convection flow connected with MHD is very important in engineering due to its wide applications, such as electromagnetic casting, liquid-metal cooling of nuclear reactors, and plasma confinement. In recent years, considerable attention has been devoted to the study of the MHD of nanofluids in natural-convection mode. Indeed, Ghasemi *et al*. [1] studied numerically by the finite volume method, the convective behavior in a differentially heated square cavity filled with nanofluid (Al_2O_3-water) and subjected to a constant horizontal magnetic field. They showed that heat transfer decreases with increasing Hartmann number and that increasing volume concentration can lead improve or decrease heat transfer depending on Hartmann number and Rayleigh number. This work by Ghasemi *et al*. [1] is

* Corresponding author, e-mail: elhattab.1970@gmail.com

followed by another study of the same problem, established by Nemat *et al*. [2] in which the Boltzmann method is used to perform the numerical simulations. The results of the investigation indicate that the mean Nusselt number improves with increasing volume fraction of nanoparticles, however the effect of nanoparticles becomes less important in the presence of a high magnetic field. Mejri *et al*. [3] presented a numerical study of natural MHD convection in a square cavity filled with a nanofluid. The vertical walls are subjected to a sinusoidal variation in temperature, while the horizontal walls are kept adiabatic. Their results show that the heat transfer rate increases with an increase in the Rayleigh number but it decreases with an increase in the Hartmann number. Another numerical study considering the same nanofluid confined in a square enclosure whose temperature of its vertical walls varies linearly, is carried out by Mahmoudi *et al*. [4]. They found that according to Hartmann number, the direction of the magnetic field controls the effects of nanoparticles. Mansour *et al*. [5] studied numerically the influence of the magnetic field on the nanofluid in natural-convection in an inclined trapezoidal cavity saturated in a porous medium of constant porosity. They have shown that an optimal heat transfer rate is obtained at higher Rayleigh values in the absence of magnetic force. Natural-convection in the presence of a magnetic field in a square cavity subjected to a temperature gradient and filled with the Cu-water nanofluid, is studied by El Hammami *et al*. [6]. The results show that the application of a magnetic field causes significant changes in flow structure and heat transfer. It causes a decrease in heat transfer and considerably reduced flow velocities. Sourtiji *et al*. [7] examined heat transfer by natural-convection in the presence of a magnetic field in a *L*-shaped cavities filled with Al_2O_3-water nanofluid. They observed that the heat transfer is augmented by adding the nanoparticles to the base fluid and increases with solid volume fraction of the nanofluid. The MHD natural-convection of Cu-water nanofluid in a skewed cavity has been studied numerically by Islam *et al*. [8]. They found that the local Nusselt number increases with the increase in the Rayleigh number and the concentration of nanoparticles. All the aforementioned works cited concern the study of the MHD of natural-convection in laminar regime. For the turbulent natural-convection MHD, we find in the literature, a numerical investigation on the laminar and turbulent convection of pure water confined in a square enclosure subjected to the influence of a uniform horizontal magnetic field conducted by Sajjadi and Kefayati [9]. Another work on the transfer of heat by convection and radiation in a turbulent flow of a nanofluid (CuO-water) subjected to the influence of a magnetic field, is carried out by Rahmati *et al*. [10]. The results show that heat transfer improves with increasing volume fraction of nanoparticles and decreases with increasing Hartmann number. Recently, Lafdaili *et al*. [11, 12] studied the heat transfer by natural turbulent convection in a 2-D and 3-D cavity filled with water containing suspended nanoparticles. They examined the effect of the form ratio and the nanoparticle type on heat transfer and flow structure.

In the present work, we numerically study the heat transfer by turbulent natural-convection of nanofluids confined in a square enclosure differentially heated and subjected to a inclined magnetic field. Numerical simulations are performed to predict the effect of Hartmann number, magnetic field orientation, Rayleigh number, volume fraction and nanoparticle type on heat transfer and flow structure.

Modelling and equations

The studied configuration is shown in fig. 1. It is a square cavity, filled with water containing different concentrations of (Cu, Al_2O_3 or TiO_2) of uniform size and shape. The cavity is formed by a left vertical wall maintained at a hot temperature, T_h, a right vertical wall maintained at a cold temperature, T_c, and two other horizontal walls considered adiabatic. The enclosure is exposed to a uniform magnetic field of intensity, B_0, oriented at an angle, γ, with

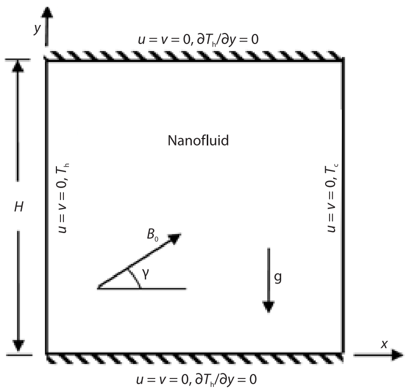

Figure 1. Physical model of the square cavity and boundary conditions

respect to the x-axis. All the thermophysical properties of nanofluids are considered constant, except for the variation in density which is estimated by the Boussinesq approximation. Table 1 shows the thermophysical properties of pure water and of the nanoparticles studied. The joule heating and viscous dissipation are neglect.

Table 1. Thermophysical properties of pure water and of the nanoparticles [6, 13]

	ρ [kgm^{-3}]	C_p [Jkg^{-1}K^{-1}]	λ [Wm^{-1}K^{-1}]	$\beta \cdot 10^{-5}$ [K^{-1}]	σ [Sm^{-1}]
Water	997	4186	0.61	27	0.05
Cu	8933	385	400	1.67	$5.96 \cdot 10^7$
Al_2O_3	3970	765	40	0.85	$35 \cdot 10^6$
TiO_2	4250	686.2	8.95	0.9	$2.6 \cdot 10^6$

To account for the effects of turbulence, the k-ε model is used. Therefore, the classical conservation equations, in the dimensionless form are written below in a cartesian co-ordinate system (x, y):

– Continuity equation

$$\frac{\partial U}{\partial X} + \frac{\partial V}{\partial Y} = 0 \tag{1}$$

– X-direction momentum equation

$$U\frac{\partial U}{\partial X} + V\frac{\partial U}{\partial Y} = -\frac{\partial P}{\partial X} + \frac{\left[\mu_{\mathrm{nf}} + \left(\mu_{\mathrm{t}}\right)_{\mathrm{nf}}\right]}{\rho_{\mathrm{nf}}\,\vartheta_{\mathrm{f}}}\sqrt{\frac{\mathrm{Pr}}{\mathrm{Ra}}}\left[\frac{\partial}{\partial X}\left(2\frac{\partial U}{\partial X}\right) + \frac{\partial}{\partial Y}\left(\frac{\partial U}{\partial Y} + \frac{\partial V}{\partial X}\right)\right] + F_{EMX} \tag{2}$$

– Y-direction momentum equation

$$U\frac{\partial V}{\partial X} + V\frac{\partial V}{\partial Y} = -\frac{\partial P}{\partial Y} + \frac{\left[\mu_{\mathrm{nf}} + \left(\mu_{\mathrm{t}}\right)_{\mathrm{nf}}\right]}{\rho_{\mathrm{nf}}\,\vartheta_{\mathrm{f}}}\sqrt{\frac{\mathrm{Pr}}{\mathrm{Ra}}}\left[\frac{\partial}{\partial Y}\left(2\frac{\partial V}{\partial Y}\right) + \frac{\partial}{\partial X}\left(\frac{\partial U}{\partial Y} + \frac{\partial V}{\partial X}\right)\right] + \frac{\beta_{\mathrm{nf}}}{\beta_{\mathrm{f}}}\theta + F_{EMY} \tag{3}$$

– Thermal energy equation

$$\begin{aligned} U\frac{\partial \theta}{\partial X} + V\frac{\partial \theta}{\partial Y} &= \frac{1}{\vartheta_{\mathrm{f}}\rho_{\mathrm{nf}}\sqrt{\mathrm{PrRa}}}\frac{\partial}{\partial X}\left[\left(\frac{\mathrm{Pr}\mu_{\mathrm{nf}}}{\mathrm{Pr}_{\mathrm{nf}}} + \frac{\mathrm{Pr}\left(\mu_{\mathrm{t}}\right)_{\mathrm{nf}}}{\sigma_T}\right)\frac{\partial \theta}{\partial X}\right] + \\ &+ \frac{1}{\vartheta_{\mathrm{f}}\rho_{\mathrm{nf}}\sqrt{\mathrm{PrRa}}}\frac{\partial}{\partial Y}\left[\left(\frac{\mathrm{Pr}\mu_{\mathrm{nf}}}{\mathrm{Pr}_{\mathrm{nf}}} + \frac{\mathrm{Pr}\left(\mu_{\mathrm{t}}\right)_{\mathrm{nf}}}{\sigma_T}\right)\frac{\partial \theta}{\partial Y}\right] \end{aligned} \tag{4}$$

– Turbulent kinetic energy equation

$$U\frac{\partial K}{\partial X}+V\frac{\partial K}{\partial Y}=\sqrt{\frac{\text{Pr}}{\text{Ra}}}\frac{1}{\rho_{\text{nf}}\vartheta_{\text{f}}}\frac{\partial}{\partial X}\left[\left(\mu_{\text{nf}}+\frac{(\mu_t)_{\text{nf}}}{\sigma_k}\right)\frac{\partial K}{\partial X}\right]+ \\ +\sqrt{\frac{\text{Pr}}{\text{Ra}}}\frac{1}{\rho_{\text{nf}}\vartheta_{\text{f}}}\frac{\partial}{\partial Y}\left[\left(\mu_{\text{nf}}+\frac{(\mu_{\text{t}})_{\text{nf}}}{\sigma_k}\right)\frac{\partial K}{\partial Y}\right]+P_k+G_k-E \tag{5}$$

– Turbulent dissipation rate equation

$$U\frac{\partial E}{\partial X}+V\frac{\partial E}{\partial Y}=\frac{1}{\rho_{\text{nf}}\vartheta_{\text{f}}}\sqrt{\frac{\text{Pr}}{\text{Ra}}}\frac{\partial}{\partial X}\left[\left(\mu_{\text{nf}}+\frac{(\mu_{\text{t}})_{\text{nf}}}{\sigma_\varepsilon}\right)\frac{\partial E}{\partial X}\right]+ \\ +\frac{1}{\rho_{\text{nf}}\vartheta_{\text{f}}}\sqrt{\frac{\text{Pr}}{\text{Ra}}}\frac{\partial}{\partial Y}\left[\left(\mu_{\text{nf}}+\frac{(\mu_{\text{t}})_{\text{nf}}}{\sigma_\varepsilon}\right)\frac{\partial E}{\partial Y}\right]+\left[C_{\varepsilon1}\left(P_k+C_{\varepsilon3}G_k\right)-C_{\varepsilon2}E\right]\frac{E}{K} \tag{6}$$

where F_{EMX} and F_{EMY} represent, respectively, the dimensionless Lorentz forces in the x- and y- directions. Their expressions are written:

$$F_{EMX}=\left(\frac{\rho_{\text{f}}}{\rho_{\text{nf}}}\right)\left(\frac{\sigma_{nf}}{\sigma_f}\right)\text{Ha}^2\sqrt{\frac{\text{Pr}}{\text{Ra}}}\left(V\sin\gamma\cos\gamma-U\sin^2\gamma\right) \tag{7}$$

$$F_{EMY}=\left(\frac{\rho_{\text{f}}}{\rho_{\text{nf}}}\right)\left(\frac{\sigma_{\text{nf}}}{\sigma_{\text{f}}}\right)\text{Ha}^2\sqrt{\frac{\text{Pr}}{\text{Ra}}}\left(U\sin\gamma\cos\gamma-V\cos^2\gamma\right) \tag{8}$$

The P_k represents the stress production and is calculated:

$$P_k=\frac{(\mu_{\text{t}})_{\text{nf}}}{\rho_{\text{nf}}\vartheta_{\text{f}}}\sqrt{\frac{\text{Pr}}{\text{Ra}}}\left[2\left(\frac{\partial U}{\partial X}\right)^2+2\left(\frac{\partial V}{\partial Y}\right)^2+\left(\frac{\partial U}{\partial Y}+\frac{\partial V}{\partial X}\right)^2\right] \tag{9}$$

The G_k is the buoyancy term, and is defined:

$$G_k=-\frac{(\mu_{\text{t}})_{\text{nf}}}{\sigma_T\rho_{\text{nf}}\vartheta_{\text{f}}}\frac{\beta_{\text{nf}}}{\beta_{\text{f}}}\sqrt{\frac{\text{Pr}}{\text{Ra}}}\frac{\partial\theta}{\partial Y} \tag{10}$$

The eddy viscosity is calculated:

$$(\mu_{\text{t}})_{\text{nf}}=\rho_{\text{nf}}C_\mu\frac{k^2}{\varepsilon} \tag{11}$$

The μ_{nf}, dynamic viscosity, of the nanofluid is evaluated using Brinkman's model [14]:

$$\mu_{\text{nf}}=\frac{\mu_{\text{f}}}{(1-\phi)^{2.5}} \tag{12}$$

where ϕ is the nanoparticle volume fraction.

The λ_{nf}, the thermal conductivity of the nanofluid is defined by the Maxwell-Garnett model [15]:

$$\lambda_{\text{nf}}=\lambda_f\left[\frac{\left(\lambda_{\text{p}}+2\lambda_{\text{f}}\right)-2\phi\left(\lambda_{\text{f}}-\lambda_{\text{p}}\right)}{\left(\lambda_{\text{p}}+2\lambda_{\text{f}}\right)+\phi\left(\lambda_{\text{f}}-\lambda_{\text{p}}\right)}\right] \tag{13}$$

The σ_{nf}, the electrical conductivity of the nanofluid is presented by Maxwell [15]:

$$\frac{\sigma_{\mathrm{nf}}}{\sigma_{\mathrm{f}}} = 1+\frac{3(\delta-1)\phi}{(\delta+2)-(\delta-1)\phi} \tag{14}$$

where $\delta = \sigma_{\mathrm{p}}/\sigma_{\mathrm{f}}$.

In eqs. (1)-(6), the dimensionless variables are used:

$$X=\frac{x}{H},\ Y=\frac{y}{H},\ U=\frac{u}{u_{\mathrm{ref}}},\ V=\frac{v}{u_{\mathrm{ref}}},\ P=\frac{p}{p_{\mathrm{ref}}},\ \theta=\frac{T-T_{\mathrm{ref}}}{T_{\mathrm{h}}-T_{\mathrm{c}}},\ E=\frac{\varepsilon}{\varepsilon_{\mathrm{ref}}},\ K=\frac{k}{k_{\mathrm{ref}}}$$
$$\mathrm{Pr}=\frac{\nu_{\mathrm{f}}}{\alpha_{\mathrm{f}}},\ \mathrm{Pr}_{\mathrm{nf}}=\frac{C_{p,\mathrm{nf}}\mu_{\mathrm{nf}}}{\lambda_{\mathrm{nf}}},\ \mathrm{Ra}=\frac{\mathrm{g}\beta_{\mathrm{f}}H^3(T_{\mathrm{h}}-T_{\mathrm{c}})}{\nu_{\mathrm{f}}\alpha_{\mathrm{f}}},\ \mathrm{Ha}=B_0H\sqrt{\frac{\sigma_{\mathrm{f}}}{\mu_{\mathrm{f}}}} \tag{15}$$

where

$$u_{\mathrm{ref}}=\sqrt{\mathrm{g}\beta_{\mathrm{f}}(T_{\mathrm{h}}-T_{\mathrm{c}})H},\ p_{\mathrm{ref}}=\rho_{\mathrm{nf}}u_{\mathrm{ref}}^2,\ T_{\mathrm{ref}}=\frac{T_{\mathrm{h}}+T_{\mathrm{c}}}{2},\ k_{\mathrm{ref}}=u_{\mathrm{ref}}^2,\ \varepsilon_{\mathrm{ref}}=\frac{u_{\mathrm{ref}}^3}{H} \tag{16}$$

To calculate the density, the coefficient of thermal expansion and the heat capacity, we use the following general relations [16]:

$$\rho_{\mathrm{nf}}=(1-\phi)\rho_{\mathrm{f}}+\phi\rho_{\mathrm{p}} \tag{17}$$

$$\beta_{\mathrm{nf}}=(1-\phi)\beta_{\mathrm{f}}+\phi\beta_{\mathrm{p}} \tag{18}$$

$$C_{p,\mathrm{nf}}=(1-\phi)C_{p,\mathrm{f}}+\phi C_{p,\mathrm{p}} \tag{19}$$

The constants in the *k*-*ε* model are:

$$C_{\mu}=0.99,\ C_{\varepsilon1}=1.44,\ C_{\varepsilon2}=1.92,\ \sigma_T=0.9,\ \sigma_k=1.0,\ \sigma_{\varepsilon}=1.3$$

The expression of $C_{\varepsilon3}$ suggested by Henkes *et al*. [17]:

$$C_{\varepsilon3}=\tanh\left|\frac{u}{v}\right| \tag{20}$$

The stream function is calculated:

$$U=\frac{\partial\psi}{\partial Y}\quad\text{and}\quad V=-\frac{\partial\psi}{\partial X} \tag{21}$$

The mean Nusselt number along the hot wall of the cavity is defined:

$$\mathrm{Nu}_m=-\frac{\lambda_{\mathrm{nf}}}{\lambda_{\mathrm{f}}}\int_0^1\frac{\partial\theta}{\partial X}\Big|_{X=0}\,\mathrm{d}Y \tag{22}$$

Numerical method and code validation

The governing equations associated with the boundary conditions are discretized by the finite volume method proposed by Patankar [18], using the power law scheme. The velocity-pressure coupling is ensured by the SIMPLE algorithm [18]. The resulting system of discretized equations is solved iteratively using the tri diagonal matrix algorithm method. The convergence criterion is defined by the formula:

$$\max\left(\frac{\left|\sum_{i=2}^{N-1}\sum_{j=2}^{M-1} R_{\Phi}\left(i,j\right)\right|}{N\times M}\right)<10^{-6} \tag{23}$$

where $R_\Phi(i, j)$ is the residual relative to the physical quantity Φ, N, and M are the number of grid points in the x- and y-directions, respectively.

In order to ensure that the numerical solution is independent of the grid, we calculated the mean Nusselt number on the hot wall for five non-uniform grids. The grid independence tests are carried out for Ra = 10^9, Ha = 0 and $\phi = 0$ and are presented in tab. 2. From this table, it appears that the 120 × 120 grid shown in fig. 2, is fine enough to perform numerical simulations.

Table 2. Result of the mean Nusselt number, and the maximum stream function, $|\psi|_{\max}$

Grid size (X×Y)	$\mathrm{Nu_m}$	Error [%]	$\lvert\psi\rvert_{\max}$	Error [%]
60×60	55.951	–	0.001618	–
80×80	56.565	1.097	0.001617	0.061
100×100	56.840	0.486	0.001609	0.494
120×120	56.995	0.272	0.001608	0.062
140×140	57.090	0.166	0.001607	0.062

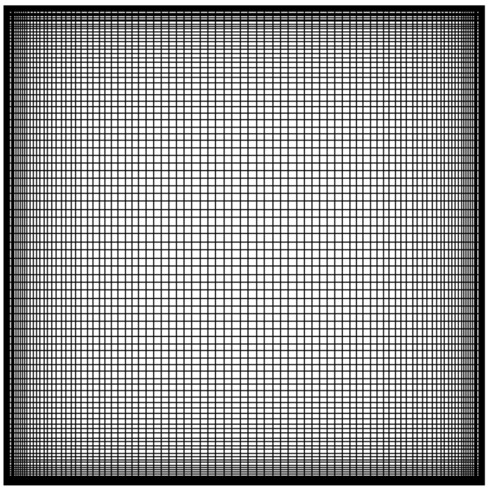

Figure 2. Grid distributions inside the domain

In order to validate our numerical code that we developed using the scientific language FORTAN90, we compared our results with those of Bairi *et al.* [19], Barakos *et al.* [20], and Dixit *et al.* [21]. The comparison concerns the mean Nusselt number along the cold wall of a cavity filled with air. Table 3 clearly shows that the works are in good agreement. Another validation was performed by comparing our results with the experimental results obtained by Ampofo and Karayiannis [22]. Figures 3(a) and 3(b) are, respectively, vertical velocity and temperature profiles at the cavity mid-height. As observed in the figures, the values of velocity profile are almost confused with the measured results. The temperature profile is also in good agreement with the measurement.

Table 3. Comparison of results obtained in this study by previous works

Ra	Present work	[19]	[20]	[21]
10^7	16.47	16.073	–	16.8
10^8	30.10	31.339	32.3	30.5
10^9	54.37	–	60.1	57.4

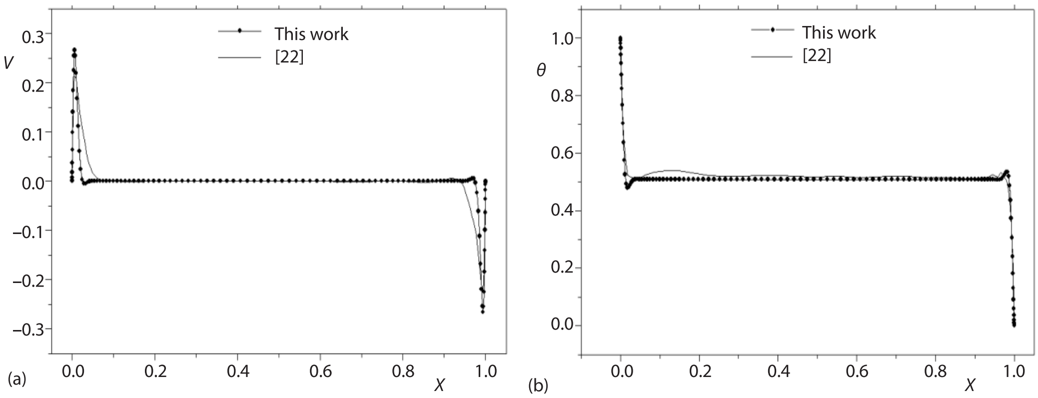

Figure 3. Comparison between present work and experimental results for $Ra = 1.58 \cdot 10^9$ and $Pr = 0.71$; (a) vertical velocity and (b) temperature at the cavity mid-height

Results and discussions

A numerical investigation was carried out to study the convective turbulent flow and heat transfer in the presence of magnetic field employing nanofluid. In this section, we discuss the numerical results obtained. This physical phenomenon is studied for a wide range of the parameter as shown in tab. 4.

Table 4. The ranges of the physical parameters

Rayleigh number	10^7 to 10^9
Hartmann number	0 to 6400
Orientation angle, γ	0° to 90°
Solid volume fraction, ϕ	0% to 6%

At $Ra = 10^9$ and without magnetic field effect (Ha = 0) the streamlines and isotherms are presented in figs. 4(a) and 4(b), respectively. These figures show that the temperature and velocity gradients have become steeper close to the vertical walls, it means that most of the flow occurs along the vertical sides of the cavity. To investigate the effect of the magnetic field, re-

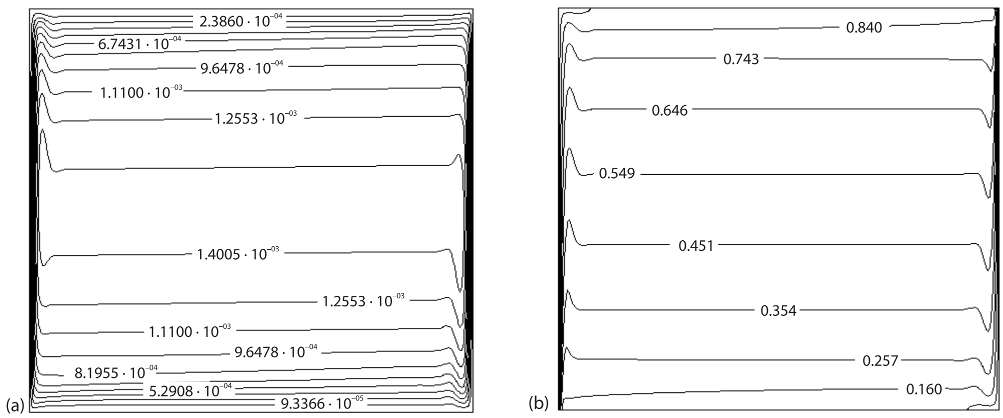

Figure 4. Streamlines (a) and isotherms (b) for $Ra = 10^9$, Ha =0 and nanofluid (water + 4%Cu)

sults illustrated in figs. 5 and 6 demonstrate the influence of magnetic field intensity (Ha = 400, 1600, and 6400) and different orientation angle of magnetic field (γ = 0°, 30°, 60°, and 90°) on the fluid-flow and the temperature distribution in the cavity. The Rayleigh number and the volume fraction of the copper nanoparticles are set at 10^9 and 0.04, respectively. The application of the magnetic field causes notable changes in the hydrodynamic and thermal structure of the flow, as shown in figs. 5 and 6. In general, as Hartmann number augments circulation strength is decreased. When $\gamma = 0°$, the magnetic field lines are horizontal and the Lorentz force F_{EMY} acts in the vertical direction and in the opposite direction to the buoyancy force, which has the effect of decelerating the circulation of the nanofluid in the cavity, the streamlines is characterized by a large main cell almost elliptical shape. When γ is increased to 90°, the magnetic field lines are vertical and the Lorentz force F_{EMX} acts in the horizontal direction and in the opposite direction of the flow, the streamlines change shape and two small swirls appear, near the right and left vertical walls. It is also observed from fig. 5, that the value of the stream function increases with the increase in the orientation of the magnetic field, this is due to the fact that when the orientation angle γ increases the horizontal component of magnetic field decreases and the vertical component increases, but the effect of the latter component is less than that of horizontal magnetic field, which improves the intensity of the flow. For low Hartmann number Ha = 400, the isotherms contours shown in fig. 6 are marked by stratification in vertical direction of the cavity and by a high temperature gradient, which shows that the heat transfer is dominated by convection. The increase in the Hartmann number leads to a decrease in the flow intensity and consequently the isotherms are transforming from convection conduction. This

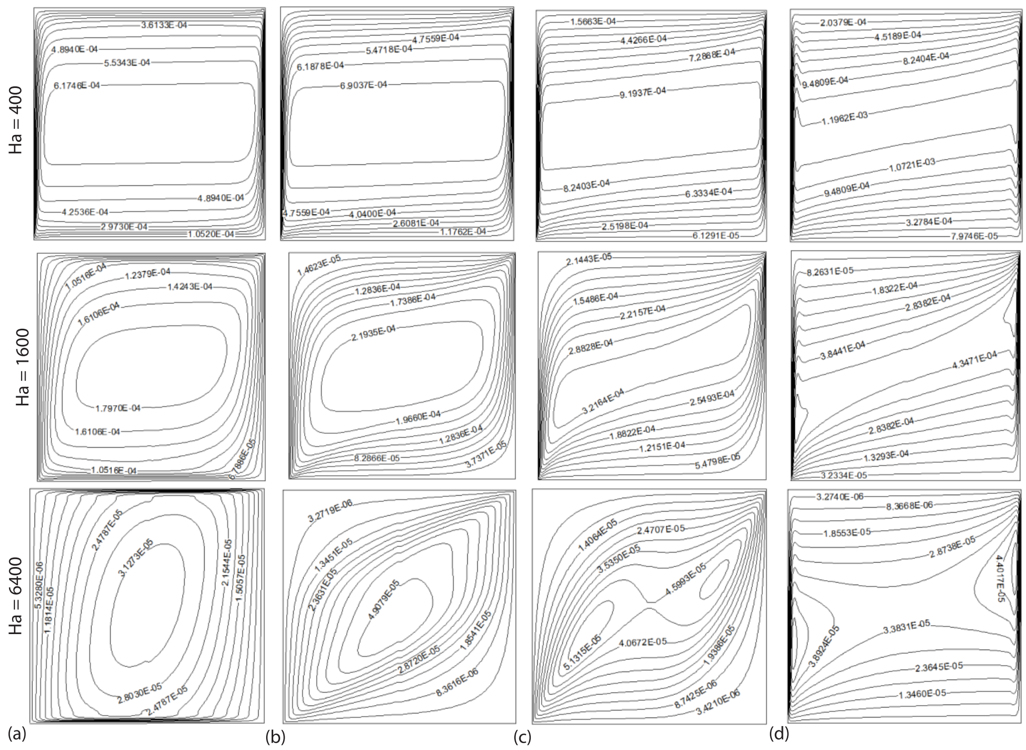

Figure 5. Streamlines for Ra= 10^9 and nanofluid (water + 4%Cu); (a) γ = 0°, (b) γ = 30°, (c) γ = 60°, and (d) γ = 90°

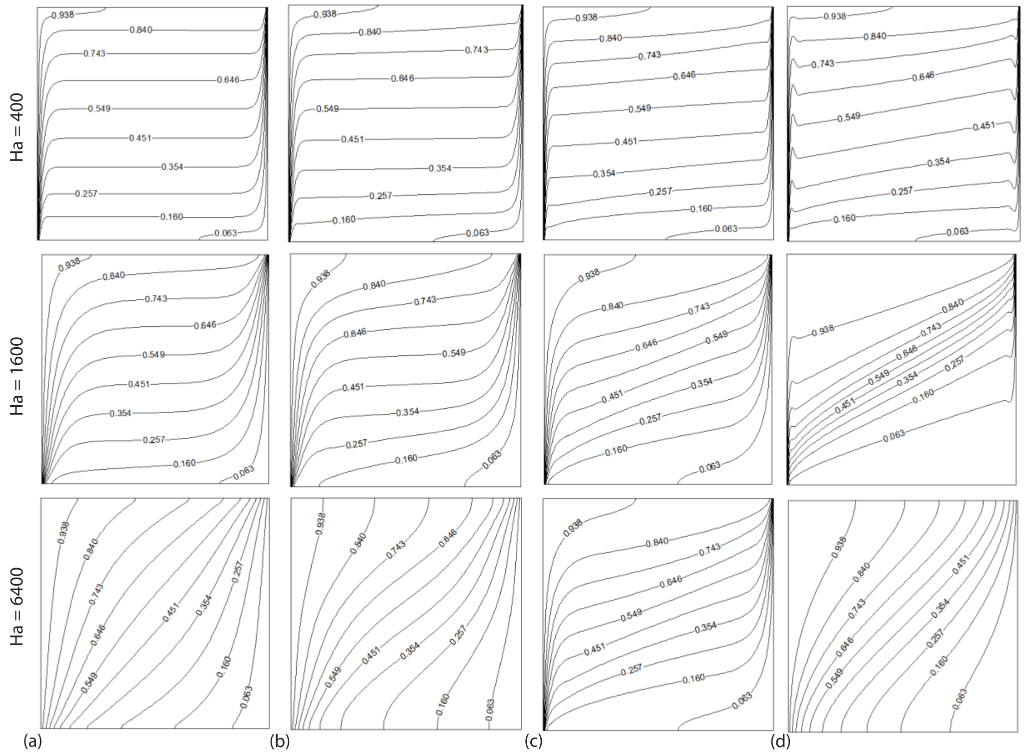

Figure 6. Isotherms for Ra= 10^9 and nanofluid (water + 4%Cu); (a) γ = 0°, (b) γ = 30°, (c) γ = 60°, and (d) γ = 90°

transformation of the isotherms is more pronounced at the high Hartmann number (Ha = 6400). The isotherms are also affected by magnetic field orientation angle γ as presented by fig. 6, the change in isotherms is very evident by comparing between γ = 0° and γ = 90° in particular for a high Hartmann number.

Figure 7 illustrates the variation of mean Nusselt number with the orientation angle of magnetic field for different Hartmann numbers when the cavity is filled with a Cu-water nanofluid (ϕ = 0.04) and the Rayleigh number is fixed at Ra = 10^9. It can be seen that, for a given orientation angle of magnetic field, the Nusselt number decreases as the Hartmann number increases. The figure shows also that the Nusselt number improves when increasing the orientation angle, but at the higher Hartmann number (Ha = 6400), the mean Nusselt number is not sensitive to the increase of the orientation angle.

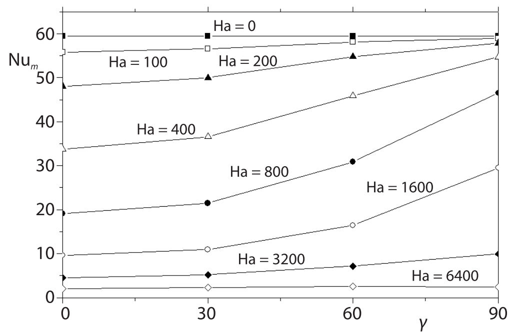

Figure 7. Variation of mean Nusselt number with γ at various Hartmann numbers for Ra = 10^9 and nanofluid (water + 4%Cu)

The variation of the mean Nusselt number as a function of the Hartmann number for different values of the orientation angle of the magnetic field is shown in fig. 8. It is noted that for all the γ values, the mean Nusselt number decreases with the increase in Hartmann number. This decrease is due to the reduction in the circulation strength as the Hartmann number increases. The mean Nusselt number increases with increasing orientation angle, but as the Hartmann number tends towards high values, the Nusselt number converges to a value of about 2.4.

Figure 9 illustrates the variation of the mean Nusselt number as a function of the Hartmann number for $\gamma = 30°$, $\phi = 0.04$ and for different Rayleigh numbers. It is clear that increase in Hartmann number decreases the mean Nusselt number. It is due to the fact that magnetic field has a negative effect on buoyancy force and it causes to slow down the flow motion. However, the mean Nusselt number increases with increasing Rayleigh number. Also, it is observed that as Hartmann number increases the Nusselt number tends to a constant value for Ra = 10^7 and 10^8.

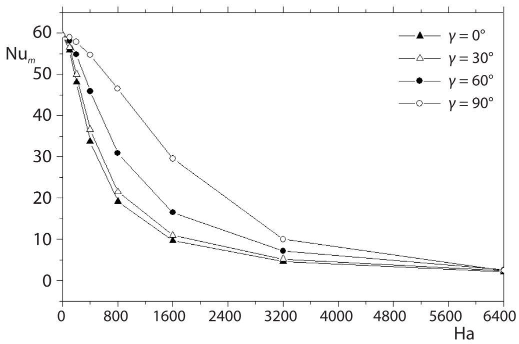

Figure 8. Variation of mean Nusselt number with Hartmann number at various orientation of the magnetic field for Ra = 10^9 and nanofluid (water + 4%Cu)

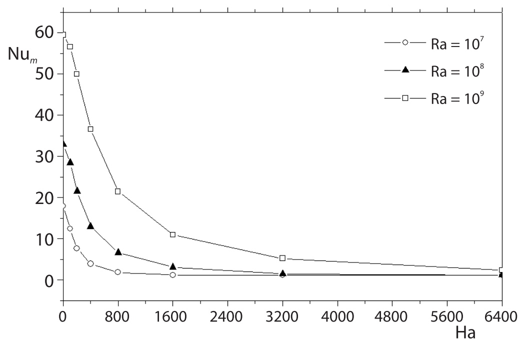

Figure 9. Variation of mean Nusselt number with Hartmann number at various Rayleigh number for $\gamma = 30°$ and nanofluid (water + 4%Cu)

We study in this paragraph, the influence of different types of nanoparticles (Cu, Al_2O_3, and TiO_2) dispersed in the base fluid on heat transfer. Figure 10 shows the variation of the mean Nusselt number as a function of the volume fraction of the nanoparticles for $\gamma = 30°$, Ha = 0, Ha = 100 and for different Rayleigh numbers. It is clear from the figure that in both cases: with and without the effect of the magnetic field, the Nusselt number increases monotonically with the increase in the volume fraction for all Rayleigh numbers and nanofluids. The highest heat transfer is obtained for Al_2O_3 since it has the lowest density in comparison with Cu and TiO_2. The heat transfer is improved also with the increase of the Rayleigh number.

The enhancement in the heat transfer provided by the nanofluid ($\phi = 0.06$) in comparison with the pure fluid ($\phi = 0$):

$$E\% = \left\{ \left[\mathrm{Nu_m}\left(\phi = 0.06\right) - \mathrm{Nu_m}\left(\phi = 0\right) \right] / \mathrm{Nu_m}\left(\phi = 0\right) \right\} \times 100$$

is shown in the tab. 5. It follows from the table that the addition of the Al_2O_3 nanoparticles in the base fluid leads to a better improvement in the heat transfer rate compared to the use of Cu or TiO_2 nanoparticles. This observation is valid either in the absence or in the presence of the magnetic field.

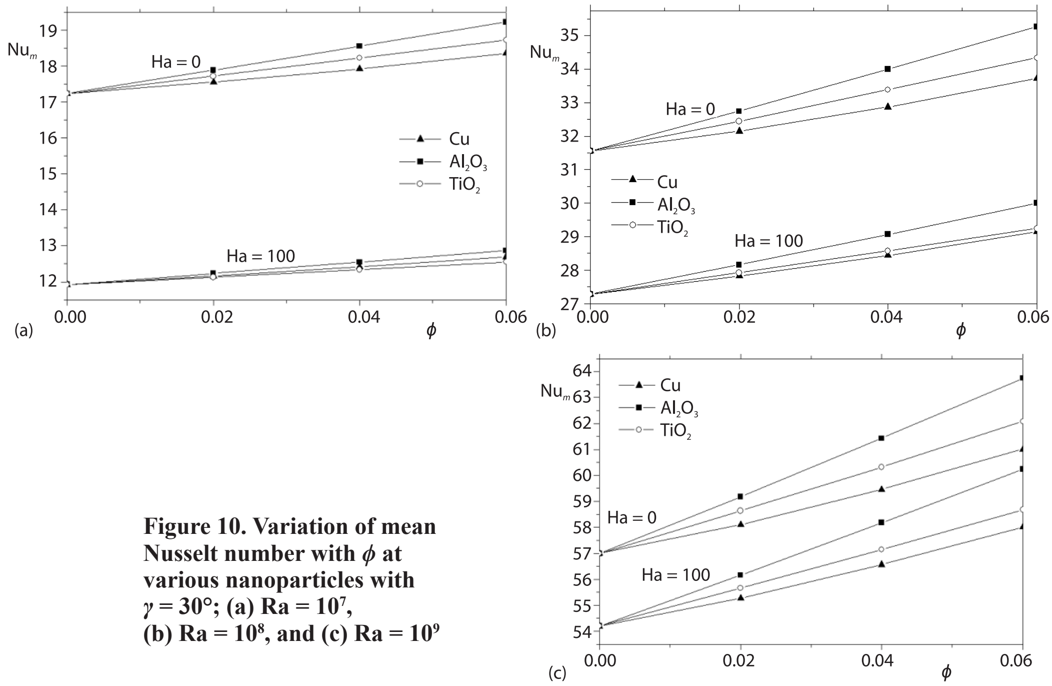

Figure 10. Variation of mean Nusselt number with ϕ at various nanoparticles with γ = 30°; (a) Ra = 10^7, (b) Ra = 10^8, and (c) Ra = 10^9

Table 5. Enhancement of the mean Nusselt number *E*% for γ = 30°

	Ra = 10^7			Ra = 10^8			Ra = 10^9		
	Cu	Al_2O_3	TiO_2	Cu	Al_2O_3	TiO_2	Cu	Al_2O_3	TiO_2
Ha = 0	6.50	11.55	8.64	6.87	11.75	8.81	7.05	11.86	8.93
Ha = 100	6.45	7.96	5.28	6.89	10.00	7.22	7.04	11.15	8.26

Conclusions

In this paper, MHD turbulent natural-convection in square cavity filled with nanofluids is numerically studied. Some important conclusions from this study can be drawn are as follows.

- The flow intensity decreases with an increase in the Hartmann number but it increases with an increase in the orientation of the magnetic field.
- The mean Nusselt number increases on increasing the orientation of the magnetic field, but at a high value of the Hartmann number, Nusselt number is not sensitive to the increase of the orientation angle.
- The mean Nusselt number increases with increasing Rayleigh number, but it decreases with an increase in the Hartmann number.
- Increasing the volume fraction of nanoparticles enhances the heat transfer.
- The type of nanoparticles is an important factor to heat transfer enhancement. The highest heat transfer is obtained when using for Al_2O_3 nanoparticles.

Nomenclature

B_0 – strength of the magnetic field, [T]
C_p – specific heat at constant pressure, [Jkg^{-1}K^{-1}]
E – dimensionless dissipation rate, [–]
G_k – buoyancy term, [Jkg^{-1}s^{-1}]
g – gravitational acceleration, [ms^{-2}]
H – cavity height, [m]

Ha – Hartmann number, [–]
K – dimensionless turbulent kinetic energy, [–]
k – turbulent kinetic energy, [m^2s^{-2}]
Nu_m – mean Nusselt number, [–]
P – dimensionless pressure, [–]
P_k – stress production term, [$Jkg^{-1}s^{-1}$]
Pr – Prandtl number, [–]
p – dimensional pressure, [Pa]
Ra – Rayleigh number, [–]
T – dimensional temperature, [K]
U, V – dimensionless velocities, [–]
u, v – velocity components, [ms^{-1}]
X, Y – dimensionless co-ordinates, [–]
x, y – cartesian co-ordinates, [m]

Greek symbols

α – fluid thermal diffusivity, [m^2s^{-1}]
β – thermal expansion coefficient, [K^{-1}]
γ – angle of the magnetic field, [°]
ε – dissipation rate, [m^2s^{-3}]
θ – dimensionless temperature, [–]
λ – thermal conductivity, [$Wm^{-1}K^{-1}$]
μ – dynamic viscosity, [Pa·s]
ν – kinematic viscosity, [m^2s^{-1}]
ρ – density, [kgm^{-3}]
σ – electrical conductivity, [Sm^{-1}]
σ_k, σ_T, σ_ε – numbers of turbulent Prandtl of k, T,
ϑ_f – kinematic viscosity of base fluid
ϕ – nanoparticle volume fraction, [–]
ψ – dimensionless stream function, [–]

Subscripts

c – cold
f – fluid (pure water)
h – hot
max – maximum
nf – Nanofluid
p – nanoparticle
ref – reference
t – turbulent

References

[1] Ghasemi, B., *et a*l., Magnetic Field Effect on Natural-Convection in a Nanofluid-Filled Square Enclosure, *International Journal of Thermal Sciences*, *5*0 (2011), 9, pp. 1748-1756
[2] Nemat, H., *et al*., Magnetic Field Effects on Natural-Convection Flow of Nanofluid in a Rectangular Cavity Using the Lattice Boltzmann, *Scientia Iranica*, *19* (2012), 2, pp. 303-310
[3] Mejri, I., *et al*., The MHD Natural-Convection in a Nanofluid-Filled Enclosure with Non-Uniform Heating on Both SideWalls, *FDMP*, *10* (2014), 1, pp. 83-114
[4] Mahmoudi, A., *et al*., The MHD Natural-Convection in a Nanofluid-Filled Cavity with Linear Temperature Distribution, *Journal of Computational Methods in Sciences and Engineering*, *14* (2014), 4, pp. 291-313
[5] Mansour, M. A., *et al*., The MHD Natural-Convection in the Localized Heat Sources of an Inclined Trapezoidal Nanofluid-Filled Enclosure, *American Journal of Engineering Research (AJER)*, *2* (2013), 9, pp. 140-161
[6] El Hammami, Y., *et al*., Numerical Study of Natural-convection of Nanofluid in a Square Enclosure in the Presence of the Magnetic Field, *International Journal of Engineering and Advanced Technology (IJEAT*), *4* (2015), 4, pp. 230-239
[7] Sourtiji, E., *et al*., Heat Transfer Augmentation of Magnetohydrodynamics Natural-Convection in L-Shaped Cavities Utilizing Nanofluids, *Thermal Science*, *16* (2012), 2, pp. 489-501
[8] Islam, T., *et al*., Numerical Study of Magnetohydrodynamic Natural-convection Heat Transfer and Fluid-flow of Nanofluid in a Skewed Cavity, *Journal of Engineering Mathematics AND Statistics*, *4* (2020), May, pp. 14-36
[9] Sajjadi, H., Kefayati, G. H. R., The MHD Turbulent and Laminar Natural-convection in a Square Cavity utilizing Lattice Boltzmann Method, *Heat Transfer – Asian Research*, *45* (2016), 8, pp. 795-814
[10] Rahmati, A. R., *et al*., Numerical Simulation of Turbulent Natural-Convection of Nanofluid with Thermal Radiation Inside a Tall Enclosure under the Influence of Magnetohydrodynamic, *Heat Transfer – Asian Research, 48* (2019), 2, pp. 520-538
[11] Lafdaili, Z., *et al*., Numerical Study of Turbulent Natural-Convection of Nanofluids in Differentially Heated Rectangular Cavities, *Thermal Science*, *25* (2021), 1B, pp. 579-589
[12] Lafdaili, Z., *et al*., Numerical Study of the Turbulent Natural-Convection of Nanofluids in a Partially Heated Cubic Cavity, *Thermal Science*, *25* (2021), 4A, pp. 2741-2754
[13] Shahzad, F., *et al*., Numerical Simulation of Magnetohydrodynamic Jeffrey Nanofuid flow and Heat Transfer over a Stretching Sheet Considering Joule Heating and Viscous Dissipation, *AIP Advances*, *8* (2018), 065316
[14] Brinkman, H. C., The Viscosity of Concentrated Suspensions and Solutions, *Journal of Chemical Physics*, *20* (1952), 4, pp. 571-581

[15] Maxwell, J. C., *A Treatise on Electricity and Magnetism*, 2nd ed., Oxford University Press, Cambridge, UK, 1904
[16] Pak, B. C., Cho, Y. I., Hydrodynamic and Heat Transfer Study of Dispersed Fluids with Submicron Metallic Oxide Particles, *Exp. Heat Transfer*, *11* (1998), 2, pp. 151-170
[17] Henkes, *et al*., Comparison of the Standard Case for Turbulent Natural-Convection in a Square Enclosure, *Proceedings*, Turbulent Natural-Convection in Enclosures: A Computational and Experimental Benchmark Study, (Eds. Henkes R. A. W. M., Hoogendoorn, C. J.), Delft, The Netheriands, 1992, pp. 185-213
[18] Patankar, S. V., *Numerical Heat Transfer and Fluid-Flow*, Hemisphere Publishing Corporation, Taylor and Francis Group., New York, USA, 1980
[19] Bairi, A., *et al*., Nusselt-Rayleigh Correlations for Design of Industrial Elements Experimental and Numerical Investigation of Natural-Convection in Tilted Square Air Filled Enclosures, *Energy Conversion and Management*, *49* (2008), 4, pp. 771-782
[20] Barakos, G., Mitsoulis, E., Natural-Convection Flow in a Square Cavity Revisited: Laminar and Turbulent Models with Wall Functions, *International Journal for Numerical Methods in Fluids*, *18* (1994), 7, pp. 695-719
[21] Dixit, H. N., *et al*., Simulation of High Rayleigh Number Convection in a Square Cavity Using the Lattice Boltzmann Method, *Int. J. Heat and Mass Transfer*, *49* (2006), 3-4, pp. 727-739
[22] Ampofo, F., Karayiannis, T. G., Experimental Benchmark Data for Turbulent Natural-Convection in an Air Filled Square Cavity, *Int. J. Heat Mass Transfer*, *46* (2003), 19, pp. 3551-3572

Paper submitted: August 25, 2021
Paper revised: September 29, 2021
Paper accepted: October 4, 2021